Influence of Tropical Pacific El Niño on the SST of the Southern Ocean through atmospheric bridge

Z.X. Li
Laboratoire de Météorologie Dynamique, CNRS, Paris, France

Abstract

El Niño is a major interannual climate signal resulting from complex ocean-atmosphere interactions in the Tropical Pacific. Its impact on the SST (Sea Surface Temperature) of the Southern Ocean through an atmospheric bridge are investigated with an atmospheric general circulation model coupled to a slab mixed-layer ocean. Simulated results suggest that SST changes in the mid- and high-latitude oceans and the Tropical Indian Ocean can be explained by modifications of heat-flux exchange at the air-sea interface. For the Tropical Atlantic, however, the discrepancy is large, indicating that the oceans dynamics are not negligible.

Introduction

It is generally recognized that El Niño results from complex ocean-atmosphere coupling in the Tropical Pacific. Although the behavior and mechanisms of El Niño are not fully understood, many successful seasonal and interannual climate predictions have been made using this major climate signal (see the review papers of *McPhaden et al.* [1998], *Neelin et al.* [1998], and the references therein). Empirical studies clearly reveal that SST (Sea Surface Temperature) anomalies of the North Pacific have a significant negative correlation with that of Tropical Pacific [e.g., *Weare et al.,* 1976; *Deser and Blackmon,* 1995]. Similar coherent structures can also be observed in other oceans.

Figure 1a shows a regression map of the global SST anomalies on the Niño-3 index (SST in the box 5°S-5°N and 92°W-150°W) for the period 1979-94. The SSTs are from the U.K. Met. Office, GISST2 [*Parker et al.,* 1995]. The regression values correspond to typical SST changes for 1°C warming of the Niño-3 SST. In the Tropical Pacific, as expected, a strong El Niño structure is obtained. We also observe negative and positive values in the North Pacific and North-West Pacific respectively. The Tropical Indian Ocean has positive values. The Tropical Atlantic has a North-South dipole structure. For the North Atlantic, positive values are found in subtropical region and negative values in high latitudes. In the Southern Oceans, positive anomalies are observed in the Indian sector and eastern part of the Pacific sector. Negative anomalies are however observed in the Atlantic sector and western portion of the Pacific sector. These features have already been noted by many authors, e.g. *Trenberth et al.* [1998].

An intriguing question is why and how do the global SST anomalies in different regions correlate to each other and particularly to El Niño ? By analyzing observed SSTs and atmospheric circulation data, *Zhang et al.* [1996] showed that the PNA (Pacific North America) pattern – a main atmospheric wave-train structure – can serve as a bridge between the tropical and extratropical North Pacific. In *Klein et al.* [1999], ship data and satellite observations were used to assess the anomalies of the atmospheric circulation and the air-sea flux exchanges. They showed that an El Niño event and its associated Southern Oscillation induce changes in cloud cover and evaporation which, in turn, alters the net flux entering other tropical basins. By using an atmospheric general circulation model, *Lau and Nath* [1994] studied the global impact when an El Niño-type SST anomaly is imposed in the Tropical Pacific, and demonstrated that the atmospheric bridge was strong enough to explain the SST correlation between the Tropical Pacific and the North Pacific. *Lau and Nath* [1996, hereafter referred to as LN96] further demonstrated that an interactive oceanic mixed-layer model could enhance this connection.

In this paper, we present a similar numerical experiment as in LN96 (TOGA-ML simulation). Our domain of interest is mainly the Southern Ocean for where there have been relatively few studies. As in LN96, utilization of slab oceanic model ensures that oceanic dynamics do not operate, and only thermodynamic interaction is taken into account. The main purpose of this paper is to quantify the role of atmospheric bridge in transferring the influence of El Niño into the Southern Ocean's surface mixed layer.

Experiments

The atmospheric model used in this study is the general circulation model of the LMD (Laboratoire de Météorologie Dynamique) – LMDZ, version 2. It is formulated in the finite-difference grid with 72 points in longitude, 45 in latitude and 19 vertical levels. A variable model-grid is used in the present study to increase slightly the horizontal resolution in the Southern Hemisphere. In contrast, the resolution in the Northern Hemisphere is coarser. A brief description of the physical parameterization and the model's main performance in simulating climate interannual variability are presented in *Li* [1999]. The model is coupled to a slab ocean of 50-meter depth. The coupling technique is similar to that used in an equilibrium CO_2 doubling experiments (see *Le Treut et al.,* [1994]). The reference heat flux is obtained through an iterative process which lasts 20 years. Once the reference heat flux with seasonal variation is obtained, it remains constant for the rest of the simulation. The control simulation (*ctrl*) is then run further for 20 years. The last 10 years are averaged and considered as equilibrium results.

To introduce the El Niño forcing, we modify the reference heat flux used in calculating the SST. First, we performed an Empirical Orthogonal Function (EOF) analysis on the SST in the Tropical Pacific basin (the box domain in Fig. 1b). The EOF structure obtained (not shown) in the form of correlation coefficient between the SST and the principal component, is then removed from the reference heat flux after multiplying a factor 30 (where the EOF value is maximum, 1 or -1, a non-equilibrium flux of 30 W m^{-2} is used). This anomaly-generation procedure is different from that of LN96 who fixed the anomaly SST pattern in the domain. An advantage of our procedure is that the discontinuity in the boundary zone is small. We will refer to this experiment as the *nino* simulation. It was also run for 20 years and the last 10 years are used to compare to the control simulation.

Figure 1b shows the SST changes from the control experiment to the perturbed El Niño experiment. In the Tropical Pacific (the box domain of Fig. 1b), we can then expect an El Niño-type SST anomaly to be obtained. Due to model internal adjustments, the resulting SST anomaly is not the exact structure of the initially-imposed EOF's structure, but is quite similar. The amplitude is roughly 50 to 100% larger than a typical El Niño event, showing that the artificially added heat-flux anomaly is too large. But this ensures a more robust signal in the model. Furthermore, from the point of view of the global average, an additional heat fluxes were added to the system which is now globally warmed.

Results

We now compare Fig. 1b against its observational counterpart, Fig. 1a. For the Southern Ocean, there are many similarities between these two maps, although simulated amplitude is larger due to the excessively imposed heat-flux anomaly. This suggests that an atmospheric bridge plays important role in connecting the SST of different oceans. For the tropical Indian basin, a warming structure is obtained for both the simulation and observations. For the Tropical Atlantic, the difference between the observation and our simulation is larger. The model gives a homogeneous warming, but the observation shows a north-south dipole structure. This discrepancy is partly due to the lack of oceanic dynamics which becomes important there. For the North Atlantic and the North Pacific, there are also important discrepancies between the simulation and the observations. This may also be explained by the lack of oceanic dynamics. But it should be regarded with caution, since there is a poor resolution in the Northern Hemisphere.

Let us now examine the variation of the heat-flux exchanges at the air-sea interface. Figure 1c shows the changes of the surface solar radiation flux in the Southern Hemisphere. It agrees well with the pattern of SST: excess (deficit) heat flux for positive (negative) SST anomaly. Further examination reveals that this is related to the changes of cloud cover (figure not shown).

The changes of cloud cover and surface solar radiation are due to changes of the atmospheric large-scale circulation, especially the modification of the planetary wave structure and the associated storm tracks. Figure 2a plots the changes of the surface wind stress from the *ctrl* simulation to the *nino* one. Figure 2b shows a similar map obtained by regressing the ERA (ECMWF re-analyse) data to the Niño-3 SST index. It can be regarded as the observational counterpart of Fig. 2a. For both the model and observations, two distinct regimes can be identified in the mid-latitude of the Southern Hemisphere, the first one in the Eastern Pacific sector where the surface wind velocity and the storm activities (deduced from the 500-hPa vertical wind) decrease; the second in the sectors of the Western Pacific, Indian and Atlantic oceans where opposite situation occurs. The primary effect of the variation on the storm track activity is to modify the cloudiness and then the radiation transfer. We should note that the surface wind variation also contributes to the changes of evaporation. Positive (negative) SST anomalies of Fig. 1b correspond roughly to a reduced (increased) surface wind (in Fig. 2a) and then evaporation.

The relationship between the convective activities of the tropics and the planetary wave and storm tracks of the high latitudes is still a non-resolved issue, although we can expect that the interaction between transient eddies and mean circulation plays an important role (see, for example, *Hoerling and Ting* [1994] and *Watanabe and Kimoto* [1999]). Let us now examine the local Hadley circulations [*Tyrrell et al.*, 1996] for two different longitude sectors. Figure 3 plots the changes of vertical velocity averaged over 60°E/130°E and 180°W/90°W respectively. We can observe that the local Hadley circulation is decreased for the Western Pacific, but increased for the Eastern Pacific.

The above described meridional circulation changes are coherent with changes of the equatorial zonal circulation. Figure 4a shows the longitude-height diagram of the zonal wind changes averaged in the equatorial band from 10°S to 10°N. Figure 4b is a similar diagram obtained by regressing the ECMWF reanalyzed wind on the Niño-3 SST index for the period 1979-93. The model's behavior is quite realistic in simulating the changes of the Walker circulation: decrease (increase) of upper (lower) wind in the Pacific sector, and the opposite situation for the Indian and Atlantic sectors. This is consistent with results found with satellite observations in *Klein et al.* [1999] (see their Fig. 4).

Concluding remarks

Using a slab ocean model coupled in an atmospheric general circulation model we have examined the coherent variation of high- and mid-latitude SST of the Southern Hemisphere in response to a Tropical Pacific perturbation. Corresponding to El Niño events, the global atmospheric circulation is modified through the changes of Walker-Hadley circulation [*Klein et al.,* 1999; *Tyrrell et al.,* 1996]. This in turn modifies the heat flux exchanges at the air-sea interface. The SST of the remote oceans thus affected. Our study is a partial coupling between atmosphere and ocean since the oceanic dynamics are neglected, and thus excluding impacts from momentum exchange at the air-sea interface. Our results help to further understand the complex behaviors of fully coupled models, and mechanisms of global teleconnection through atmospheric bridges.

Our findings are consistent with those of LN96 and *Klein et al.,* [1999], and quite realistic compared to observations in the Southern Oceans. However, for the Tropical Atlantic the discrepancy between observations and simulation is important. We suspect that the Tropical Atlantic does not passively respond to El Niño, and its own dynamics need to be correctly taken into account. For mid and high latitudes, the SST shows a more passive role [*Frankignoul,* 1985], and responds mainly to tropical variation (in particular, Tropical Pacific) through the atmospheric teleconnection mechanisms. Further studies are needed to evaluate influences of these high-latitude SST anomalies on the atmospheric circulation in order to understand the full feedback loop of the climate system.

Acknowledgments. This work is supported by the Environment Program of the European Commission through the SINTEX project. Comments from Peter Gleckler, Bryan Weare and two anonymous referees helped to clarify many points of the text.

References

Deser, C., and M. L. Blackmon, On the relationship between tropical and north Pacific sea surface temperature variations, *J. Climate, 8*, 1677-1680, 1995.

Frankignoul, C., Sea surface temperature anomalies, planetary waves and air-sea feedbacks in the middle latitude, *Rev. of Geophys., 23*, 357-390, 1985.

Hoerling, M. P., and M. Ting, Organization of extratropical transients during El Niño, *J. Climate, 7*, 745-766, 1994.

Klein, S. A., B. J. Soden, and N.-C. Lau, Remote Sea Surface Temperature variations during ENSO: Evidence for a tropical atmospheric bridge, *J. Climate, 12*, 917-932, 1999.

Lau, N. C., and M. J. Nath, A modeling study of the relative roles of tropical and extratropical SST anomalies in the variability of the global atmosphere-ocean system, *J. Climate, 7*, 1184-1207, 1994.

Lau, N. C., and M. J. Nath, The role of the Atmospheric Bridge in linking tropical Pacific ENSO events to extratropical SST anomalies, *J. Climate, 9*, 2036-2057, 1996.

Le Treut, H., Z. X. Li, and M. Forichon, Sensitivity of the LMD general circulation model to greenhouse forcing associated with two different cloud water parameterizations, *J. Climate, 7*, 1827-1841, 1994.

Li, Z. X., Ensemble atmospheric GCM simulation of climate interannual variability from 1979 to 1994, *J. Climate, 12*, 986-1001, 1999.

McPhaden, M. J., A. J. Busalacchi, R. Cheney, J.-R. Donguy, K. S. Gage, D. Halpern, M. Ji, P. Julian, G. Meyers, G. T. Mitchum, P. P. Niiler, J. Picaut, R. W. Reynolds, N. Smith, and Kensuke Takeuchi, The Tropical Ocean-Global Atmosphere observing system: A decade of progress, *J. Geophys. Res., 103*, 14169-14240, 1998.

Neelin, J. D., D. S. Battisti, A. C. Hirst, F.-F. Jin, Y. Wakata, T. Yamagata, and S. E. Zebiak, ENSO theory, *J. Geophys. Res., 103*, 14261-14290, 1998.

Parker, D. E., M. Jackson, and E. B. Horton, The GISST2.2 sea surface temperature and sea-ice climatology, Climate Research Technical Note 63, Hadley Centre, Meteorological Office, Bracknell, U.K., 35pp, 1995.

Trenberth, K. E., G. W. Branstator, D. Karoly, A. Kumar, N.-C. Lau, and C. Ropelewski, Progress during TOGA in understanding and modeling global teleconnections associated with tropical sea surface temperatures, *J. Geophys. Res., 103*, 14291-14324, 1998.

Tyrrell, G. C., D. Karoly, and J. L. McBride, Links between tropical convection and variations of the extratropical circulation during TOGA COARE, *J. Atmos. Sci., 53*, 2735-2748, 1996.

Watanabe, M., and M. Kimoto, Tropical-extratropical connection in the Atlantic atmosphere-ocean variability, *Geophys. Res. Lett., 26*, 2247-2250, 1999.

Weare, B. C., A. Navato, and R. E. Newell, Empirical orthogonal analysis of Pacific Ocean sea surface temperatures, *J. Phys. Oceanogr., 6*, 671-678, 1976.

Zhang, Y., J. M. Wallace, and N. Iwasaka, Is climate variability over the North Pacific a linear response to ENSO?, *J. Climate, 9*, 1468-1478, 1996.

Z.X. Li, LMD/CNRS, case courrier 99, Université

Pierre et Marie Curie, 4 Place Jussieu, 75252 Paris cedex 05, France. (e-mail: li@lmd.jussieu.fr)

October 27, 1999; revised August 21, 2000; accepted August 23, 2000.

This preprint was prepared with AGU's LaTeX macros v4. File bb formatted October 18, 2000.

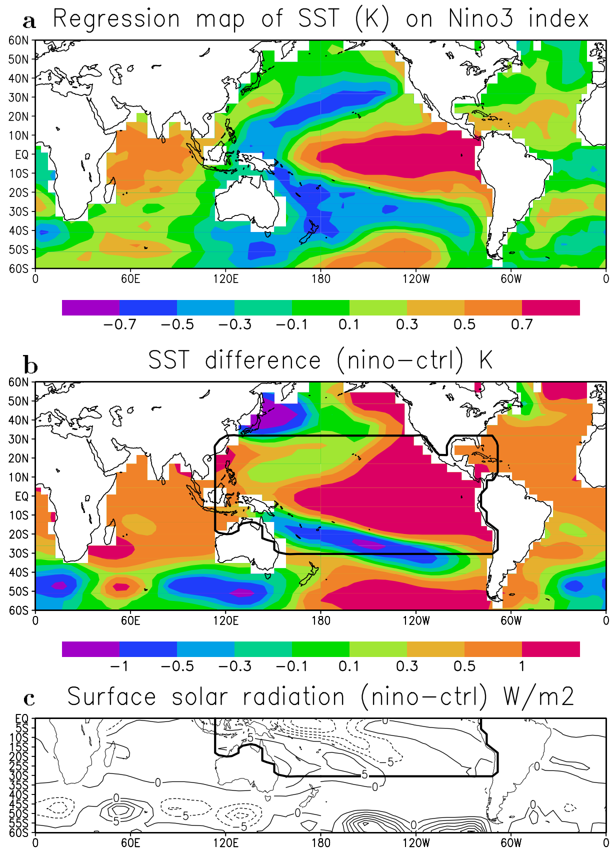

Figure 1. (a) Regression map of the global SST on the SST of Niño-3 region (5°S-5°N, 92-120°W). Results are obtained for the period 1979-94. (b) Annual-mean SST differences between the perturbed (*nino*) simulation and the control (*ctrl*) one. Unit is K for both (a) and (b). (c) Differences (W m^{-2}) of surface solar radiation flux between the perturbed and control simulations.

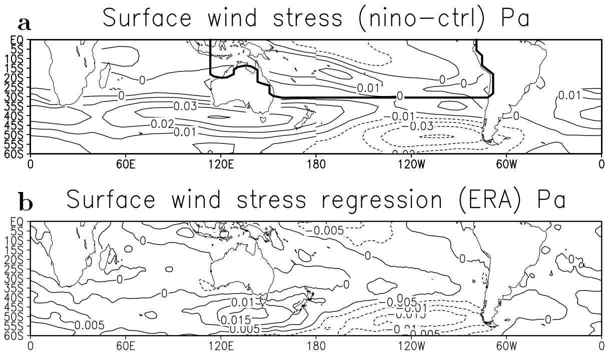

Figure 2. (a) Differences (Pa) of the surface wind stress between the perturbed and control simulations. (b) Regressed map (unit is Pa) of the ECMWF reanalyzed surface wind stress on the Niño-3 SST index for the period 1979-93.

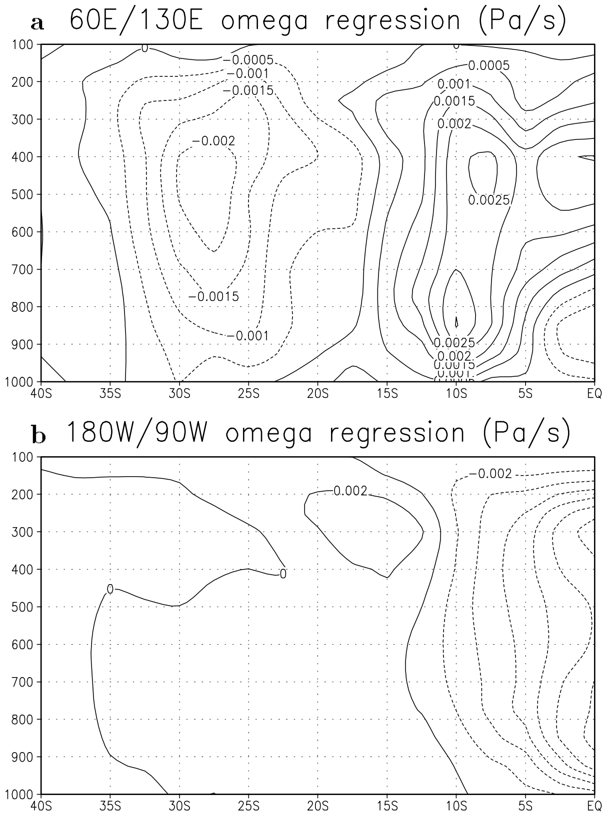

Figure 3. Latitude-height diagrams showing the regressed values (Pa s^{-1}) of the observed vertical wind on the Niño-3 SST index for the period 1979-93. Top panel is for the sector of the Indian and Western Pacific oceans, and the bottom one the Eastern Pacific sector. Negative values indicate upward movement, positive values downward movement.

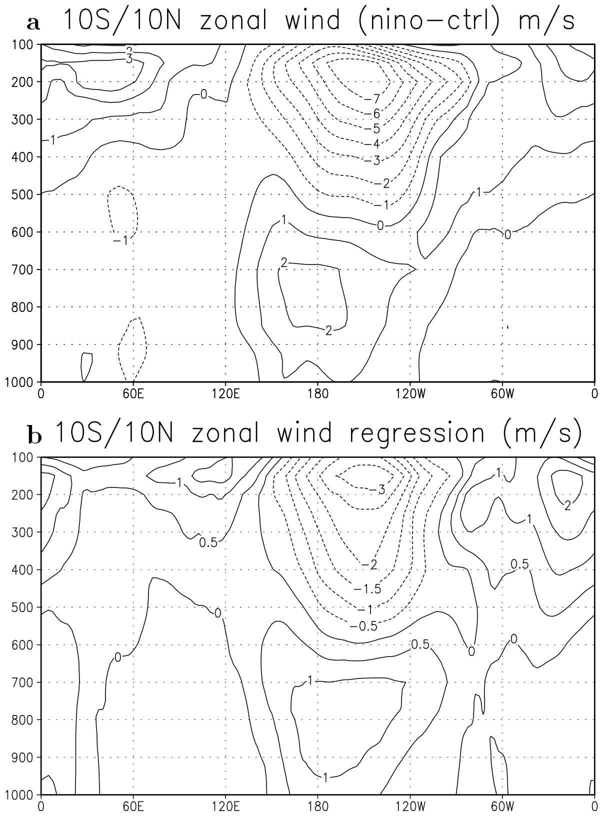

Figure 4. (a) Longitude-height diagram showing the difference (*nino* minus *ctrl*) of the zonal wind (m s^{-1}) in the 10°S/10°N equatorial band. (b) Regressed values (m s^{-1}) of the observed zonal wind in the equatorial band on the Niño-3 SST index for the period 1979-93.